Inorg. Chem. **2009**, *48*, 4549−4556

Palladium Diselenolenes: a New Group of near-Infrared Lumophores

Karen Rofe,*,† Peter Douglas,*,† Christopher P. Morley,‡ Christopher A. Webster,§ and Jeremie G. Pichereau†

Chemistry Group, School of Engineering, Swansea University, Singleton Park, Swansea SA2 8PP, U.K., School of Chemistry, Cardiff University, P.O. Box 912, Cardiff CF10 3AT, U.K., and Celtic Chemicals Ltd., Unit 25 Kenfig Industrial Estate, Margam, Port Talbot SA13 2PE, U.K.

Received September 3, 2008

We describe the photochemical characteristics of two phosphorescent palladium diselenolenes $[Pd_2(Se_2C_8H_{12})_2(PBu_3)_2]$ (**1**) and $[Pd_2(Se_2C_8H_{12})_2(PPh_3)_2]$ (**2**) which, to the best of our knowledge, are the first reported examples of luminescent Pd−Se compounds. Both compounds exhibit broadband near-infrared phosphorescence in the solid state, with λ_{max} of 717 nm for **1** and 792 nm for **2** at 298 K, and 752 nm for **1** and 785 nm for **2** at 77 K. No phosphorescence was detected for either compound when they were dissolved in nitrogen-purged acetonitrile or toluene solution at 298 K but they do phosphoresce at 77 K in organic glasses with emission quantum yields of 0.12 (±0.01) for **1** and 0.13 (±0.01) for **2** in an ethanol/diethylether/toluene (1:2:1) (EDT) glass. Emission lifetimes at 77 K are the same whether in the solid state or in an organic glass with first order fit lifetimes of $\tau = 18.8$ (±0.7) μs and 11.5 (±0.3) μs for **1** and **2**, respectively. Combination of these lifetimes with quantum yields gives radiative lifetimes of 151 (±13) μs and 86 (±7) μs for compounds **1** and **2**, respectively, at 77 K in EDT glass. At 77 K solid state quantum yields are estimated to be of the same order of magnitude as those in glasses, and these decrease by a factor of about 3−5 in going from 77 to 298 K. In the solid state at 298 K emission lifetimes are 1.83 (±0.02) μs and 7.0 (±0.3) μs for **1** and **2**, respectively. We could detect no transients by nanosecond flash photolysis which could be assigned to the triplet state in room temperature solution, and no emission assignable to singlet oxygen across the wavelength range 1200−1350 nm upon 550 nm excitation of either **1** or **2** in acetonitrile solution. We estimate the quantum yield of singlet oxygen formation to be less than about 5×10^{-4}, which is also an upper limit for the yield of triplet states of any significant lifetime in fluid solution. Density functional theory (DFT) calculations of the S_0 to S_1 and T_1 transitions show a shift in molecular orbital character from one with significant -ene π involvement but very little P involvement in the ground-state to one with less −ene π but greater P involvement in the excited states; there is also a significant shift in the distribution of involvement of atomic orbitals on the four Se atoms.

Introduction

Over the past 25 years the optical properties of a number of transition metal compounds have been investigated because of their potential technological applications as visible and near-infrared absorbers and emitters in systems such as organic light-emitting diodes, molecular electronics, and sensors.[1−8] Much effort has concentrated on second and third row transition metals where heavy atom effects enhance both singlet to triplet intersystem crossing and radiative decay

* To whom correspondence should be addressed. E-mail: karenrofe@hotmail.com (K.R.), p.douglas@swansea.ac.uk (P.D.).
† Swansea University.
‡ Cardiff University.
§ Celtic Chemicals Ltd.

(1) Ford, S.; Morley, C. P.; Di Vaira, M. *Inorg. Chem.* **2004**, *43*, 7101–7110.
(2) Lau, K. L.; Cheung, K. M.; Zhang, Q. F.; Song, Y.; Wong, W. K.; Williams, I. D.; Leung, W. A. *J. Organomet. Chem.* **2004**, *689*, 2401–2410.
(3) Baldo, M. A.; Lamansky, S.; Thompson, M. E.; Forrest, S. R. *Appl. Phys. Lett.* **1999**, *75*, 4–6.
(4) McGarrah, J. E.; Kim, Y.; Hissler, M.; Eisenberg, R. *Inorg. Chem.* **2001**, *40*, 4510–4511.
(5) Pyle, A. M.; Rehmann, J. P.; Meshoyer, R.; Kumar, C. V.; Turro, N. J.; Barton, J. K. *J. Am. Chem. Soc.* **1988**, *111*, 3051–3058.
(6) Preininger, C.; Kilmant, I.; Wolfbeis, O. S. *Anal. Chem.* **1994**, *66*, 1841–1846.
(7) Rosace, G.; Giuffrida, G.; Saitta, M.; Guglielmo, G.; Campanga, S.; Lanza, S. *Inorg. Chem.* **1996**, *35*, 6816–6822.
(8) Evans, R. C.; Douglas, P.; Winscom, C. J. *Coord. Chem. Rev.* **2006**, *250*, 671–774.

10.1021/ic801694r CCC: $40.75 © 2009 American Chemical Society
Published on Web 04/20/2009

from the resulting triplet states.[8−20] For the group 10 elements most reports deal with the remarkable luminescent properties of Pt(II) complexes, and there are relatively few reports dealing with luminescent Ni(II) and Pd(II) complexes.[17−26] It has been suggested that the lack of luminescent Pd(II) complexes is a consequence of the low lying energy levels of the d-d excited states in Pd(II) in comparison to Pt(II).[21,22]

Several types of luminescent sulfur-containing transition metal compounds have been reported.[1,18,19] Eisenberg and co-workers have investigated many Pt(II) complexes possessing either a dithiolate or a dithiocarbamate ligand, which show red emission in solution and in the solid state,[4] but related Pd(II) complexes have not received much attention. Furthermore, studies of complexes of analogous ligands based on the heavier chalcogens with either Pt or Pd are rare even though organoselenium compounds have a strong affinity toward the heavy transition metals, possibly because until recently there has been a lack of generally applicable preparative methods for such compounds.[1,27]

The reactions of 1,2,3-selenadiazoles with low-valent transition metal complexes have been used to prepare a wide range of selenium-containing compounds. In previous work some of us reported the reaction of bis(cycloalkeno)-1,4-diselenins (which are prepared from 1,2,3-selenadiazoles) with a tributyl- or triphenyl- phosphinepalladium(0) precursor, which resulted in two novel palladium diselenolenes, namely $[Pd_2(Se_2C_8H_{12})_2(PBu_3)_2]$ **1** and $[Pd_2(Se_2C_8H_{12})_2(PPh_3)_2]$ **2**, Figure 1.[26,27]

Further examination of these compounds showed them to be luminescent, and here we report the photochemical characterization of these compounds, which are, to the best of our knowledge, the first examples of luminescent Pd(II) selenium compounds in the literature.

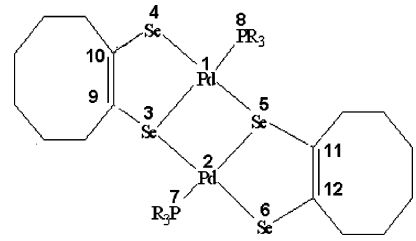

Figure 1. Structures of **1** (R = butyl) and **2** (R = phenyl). The atom numbering is that used in the text and Figure 11.

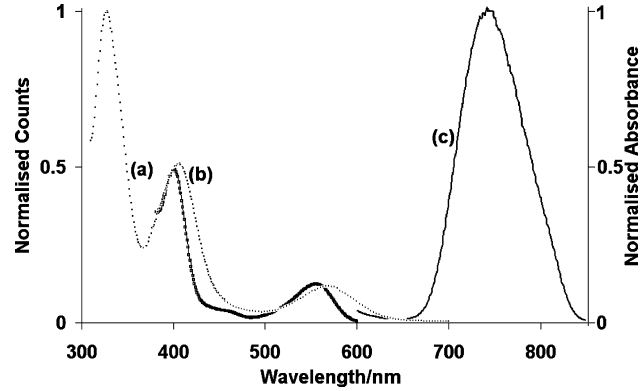

Figure 2. Spectra of **1** in MCH solution and 77 K glass. (a) Absorption in RT solution; (b) excitation for 747 nm emission in 77 K glass; (c) emission for 445 nm excitation in 77 K glass.

Experimental Section

Compounds **1** and **2** were prepared as previously described,[26,27] and their structures confirmed by NMR spectroscopy and mass spectrometry. **1** is a purple solid and gives red solutions; **2** is a dark green solid and gives green solutions.

Materials and General Procedures. All the reactions involved in the preparations of **1** and **2** were performed using standard Schlenk techniques under an atmosphere of dry nitrogen. Acetonitrile (Fisher or Reidel-de Haen), diethylether (Fisher or BDH), ethanol (Fisher, or Jose Manuel Gomes Dos Santos LDA), methylcyclohexane (MCH) (Fisher spectroscopic grade), and toluene (Fisher, or Merck spectroscopic grade) were used as supplied. Tetraphenylporphyrin (TPP) was obtained from Alfa Aesar and 9*H*-fluoren-9-one was a gift from J. Pina, Departmento de Quimica, Universidade de Coimbra, Portugal.

Methods. Absorption Spectroscopy. UV−visible spectra were recorded using either a Unicam UV300 spectrometer or an HP 8452A diode array spectrophotometer. The molar extinction coefficients were obtained from absorption measurements using six solutions of different concentrations in quartz absorption cuvettes ranging from 1 mm to 10 cm path length. Experimental oscillator strengths, f_{exp}, were calculated from $f_{exp} = 4.3 \times 10^{-9} \int \varepsilon d\upsilon$, where $\int \varepsilon d\upsilon$ is the area under the curve of the molar extinction coefficient plotted against wavenumber.[28]

Emission Spectroscopy. Room temperature (RT) and 77 K emission measurements were carried out using either a Perkin-Elmer MPF-44E fluorescence spectrometer or a Horiba-Jobin-Ivon SPEX Fluorog 3-22 spectrometer. 2 nm excitation and 5 nm emission slits

(9) Miskowski, V. M.; Houlding, V. H.; Che, C. M.; Wang, Y. *Inorg. Chem.* **1993**, *32*, 2518–2524.
(10) Barigelletti, F.; Sandrini, D.; Maestri, M.; Balzani, V.; Zelewsky, A.; Chassot, L.; Jolliet, P.; Maeder, U. *Inorg. Chem.* **1998**, *27*, 3644–3642.
(11) Graham, L. W.; Heath, G. A.; Krausz, E.; Moran, G. *Inorg. Chem.* **1991**, *30*, 347–349.
(12) Thomas, J.; Lin, J. T.; Lin, H.; Chang, C.; Chuen, C. *Organometallics* **2001**, *20*, 557–563.
(13) Laskar, I. R.; Hsu, S.; Chen, T. *Polyhedron* **2005**, *24*, 198–200.
(14) Gao, F. G.; Bard, A. J. *Chem. Mater.* **2002**, *14*, 3465–3470.
(15) Collin, J.; Dixon, I. M.; Sauvage, J.; Williams, J. A. G.; Barigelletti, F.; Flamigni, L. *J. Am. Chem. Soc.* **1999**, *121*, 5009–5016.
(16) Hao, L.; Lachicotte, R. J.; Gysling, H. J.; Eisenberg, R. *Inorg. Chem.* **1999**, *38*, 4616–4617.
(17) Gellene, G. I.; Roundhill, D. M. *J. Phys. Chem. A* **2002**, *106*, 7617–7620.
(18) Bevilacqua, J. M.; Zuleta, J. A.; Eisenberg, R. *Inorg. Chem.* **1994**, *33*, 258–266.
(19) Paw, W.; Connick, W. B.; Eisenberg, R. *Inorg. Chem.* **1998**, *37*, 3919–3926.
(20) Carlson, B.; Phelan, G. D.; Kaminsky, W.; Dalton, L.; Jiang, X.; Liu, S.; Jen, A. *J. Am. Chem. Soc.* **2002**, *124*, 14162–14172.
(21) Ma, Y.; Zhang, H.; Shen, J.; Che, C. *Synth. Met.* **1998**, 245–248.
(22) Zipp, A. P. *Coord. Chem. Rev.* **1988**, *84*, 47–83.
(23) Bevilacqua, J. M.; Eisenberg, R. *Inorg. Chem.* **1994**, *33*, 2913–2923.
(24) Akawa, M.; Kanbara, T.; Fukumoto, H.; Yamamoto, T. *J. Organomet. Chem.* **2008**, *690*, 4192–4196.
(25) (a) Ford, S.; Khanna, P. K.; Morley, C. P.; Di Vaira, M. *J. Chem. Soc., Dalton Trans.* **1999**, 791–794 (Crystal structure CCDC ref. no. 186/1317). (b) Ford S. New palladium complexes containing organoselenium ligands. PhD Thesis, University of Wales, Swansea, U.K., 2000.
(26) Ford, S.; Lewtas, M. R.; Morley, C. P.; Di Vaira, M. *Eur. J. Inorg. Chem.* **2000**, 933–938.
(27) Ford, S.; Morley, C. P.; Di Vaira, M. *New J. Chem.* **1999**, *23*, 811–813.
(28) Turro, N. J. *Modern Molecular Photochemistry*; University Science Books: Sausalito, CA, 1999; p 89.

Table 1. Absorption Maxima, Extinction Coefficients, and Oscillator Strengths for **1** and **2** in Various Solvents

	solvent								
	EDT		MCH			acetonitrile		toluene	
compound	λ_{abs}/nm	ε /10^4 M^{-1} cm^{-1}	λ_{abs}/nm	ε /10^4 M^{-1} cm^{-1}	f	λ_{abs}/nm	ε /10^4 M^{-1} cm^{-1}	λ_{abs}/nm	ε /10^4 M^{-1} cm^{-1}
1	291	2.41 ± 0.09	285	2.34 ± 0.05		291	2.21 ± 0.03	292	2.31 ± 0.03
	326	1.43 ± 0.05	330	1.38 ± 0.03	0.228	327	1.32 ± 0.02	328	1.25 ± 0.02
	405 (409)[a]	0.71 ± 0.02	409 (403)[a]	0.68 ± 0.01	0.098	404	0.66 ± 0.02	406	0.66 ± 0.01
	574 (579)[a]	0.14 ± 0.01	573 (576)[a]	0.13 ± 0.01	0.018	583	0.12 ± 0.01	566	0.12 ± 0.01
2	334	2.61 ± 0.09	328	2.50 ± 0.02	0.700	341	2.24 ± 0.02	326	3.31 ± 0.02
	443 (449)[a]	2.52 ± 0.06	436	0.78 ± 0.01	0.117	427	0.61 ± 0.01	436	0.74 ± 0.01
	573 (578)[a]	1.48 ± 0.04	596	0.12 ± 0.01	0.019	591	0.11 ± 0.01	590	1.18 ± 0.01

[a] Wavelengths in brackets are corresponding maxima in excitation spectra.

were used for excitation spectra, and 5 nm excitation and 2 nm emission slits were used for emission spectra. For room temperature solution measurements a 1 cm × 1 cm quartz fluorescence cell was used. For 77 K measurements the sample was held in a quartz tube of about 3 mm diameter and placed in liquid nitrogen in a phosphorescence Dewar flask. For measurements using frozen toluene the MPF-44E fluorimeter was used, while for all others the SPEX Fluorog 3-22 spectrometer was used. Fluorescence spectra measured using the SPEX Fluorog 3-22 were obtained in photon counting mode and automatically corrected for detector wavelength response using manufacturer's correction files. Two organic glasses were used: ethanol/diethylether/toluene (1:2:1) (EDT), which is relatively polar, and methylcyclohexane (MCH), which is non-polar.[29]

Quantum yields for emission in 77 K EDT glasses were measured with the SPEX Fluorog 3-22 spectrometer using TPP in EDT as emission standard ($\Phi_{em} = 0.15$ in ethanol;[30] $\Phi_{em} = 0.14$ in EDT, at both 77 and 298 K (this work)). The method of comparison used was as follows. Sample and reference solutions in EDT of comparable absorption were prepared, and excitation wavelengths chosen where their absorbances were the same at about 0.3 in a 1 cm path length cell (these were 496 and 523 nm). The spectra of both the sample solution and the reference were then obtained at 77 K using these excitation wavelengths. The reference solution was then allowed to warm to room temperature, and the emission spectrum was recorded again. This gave four emission ratios: two with both sample and reference at 77 K; and two with sample at 77 K and reference at room temperature. The emission quantum yield, Φ_X, of sample X was calculated by reference to the standard R using eq 1 below. A is the intensity of light absorbed at the excitation wavelength, I is the integrated emission intensity corrected for the instrument response, and n is the refractive index of the solvent.[31]

$$\Phi_X = \Phi_R(A_R/A_X)(I_X/I_R)(n_X/n_R)^2 \quad (1)$$

Both the sample and the reference were excited at the same wavelength. For the calculation of sample absorbances at 77 K from room temperature spectra, we have used a contraction value of 80% for EDT in going from RT to 77 K, which is typical for most organic glasses.[30] We also note that at the excitation wavelengths used the solution phase absorption spectra and 77 K glass excitation spectra of **1** and **2** are quite flat and environment independent.

Laser Kinetic Emission Spectroscopy. Laser kinetic emission measurements were obtained using an Applied Photophysics laser kinetic spectrometer with either the 355 or the 532 nm emission from a Spectron Nd/YAG laser as excitation pulse. A Hamamatsu R928 photomultiplier, emission slits of 19 nm, a 644 nm wavelength cutoff filter, and a 1 kΩ load terminator on the emission detection system were used for all measurements. For 77 K glasses and 77 K solids the averaged data from four decay curves were recorded using a LeCroy 9304AM oscilloscope. For RT solids, which gave a weaker signal, averaging was increased to sixteen shots and the laser amplifier used to improve the signal-to-noise ratio. The kinetic data were analyzed using Jandel Table-Curve, and in those cases where a large pulse signal from scatter or adventitious fluorescence was apparent, curve fitting was carried out ignoring that initial distorted portion of the signal, which was typically the first 0.5−1 μs.

Laser Kinetic Absorption Spectroscopy. Transient difference absorption spectra were obtained using an Applied Photophysics laser kinetic spectrometer with the third harmonic, 355 nm, of a Nd/YAG laser (Spectra Physics) as excitation source.

Singlet Oxygen Measurements. Attempts to measure room temperature singlet oxygen phosphorescence were carried out using the SPEX Fluorog 3−22 spectrometer with a 600-line diffraction grating monochromator, and a Hamamatsu R5509−42 photomultiplier cooled to 77 K in a liquid nitrogen chamber (Products for Research model PC176TSCE-005) with a Schott RG665 filter to eliminate all the first harmonic contributions from the sensitizer emission in the 500−800 nm region from the infrared signal. 9*H*-Fluoren-9-one in ethanol was used as reference.[31]

Computation. Calculations were performed with the Gaussian 03 suite of programs. Geometry optimizations were carried out at the B3LYP/6-21G(d,p) level, with the LANL2DZ valence functions and effective core potentials for the Pd and Se atoms.

Results and Discussion

Absorption Spectroscopy. Both compounds dissolve readily in MCH, acetonitrile, toluene, and EDT. Throughout this study we found no obvious signs of aggregation in solution. Both compounds gave linear Beer−Lambert plots in MCH across the concentration range 1.5×10^{-7} to 1×10^{-4} M. Absorption data are shown in Table 1, and Figures 2 and 3 give the absorption spectra of **1** and **2** in MCH. Absorption spectra in the visible and near UV are characterized by three distinct transitions of decreasing intensity with increasing wavelength. The relatively high extinction coefficients indicate spin-allowed transitions. The two visible absorption maxima of **2** are shifted to longer wavelength by up to about 30 nm compared to those of **1**; a difference in energy, depending upon solvent, of 1200−2100 cm^{-1} for the 400/450 nm bands, but much less, 30−700 cm^{-1}, for the 570/600 nm bands.

(29) Montalti, M.; Credi, A.; Prodi, L.; Gandolfi, M. T. *Handbook of Photochemistry*, 3rd ed.; CRC Press: New York, 2006.
(30) Lakowicz. J. R. *Principles of Fluorescence Spectroscopy*, 2nd ed.; Kluwer Academic: New York, 1999.
(31) Martinez, C. G.; Neuner, A.; Marti, C.; Nonell, S.; Braun, A. M.; Oliveros, E. *Helv. Chim. Acta* **2003**, *86*, 384–397.

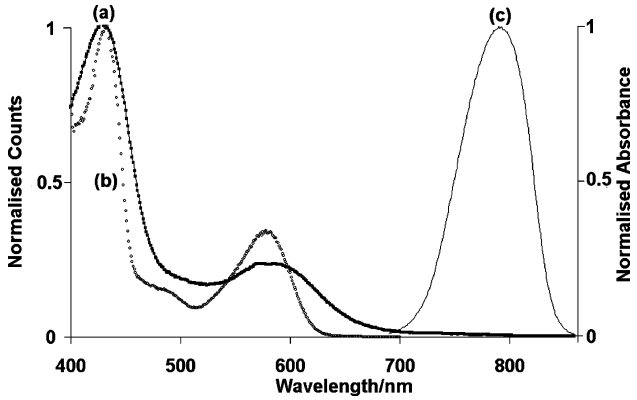

Figure 3. Spectra of **2** in MCH RT solution and 77 K glass. (a) Absorption in RT solution; (b) excitation for 747 nm emission in 77 K glass; (c) emission for 420 nm excitation in 77 K glass.

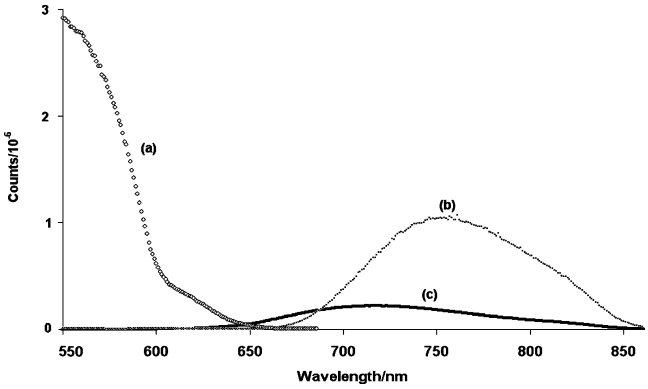

Figure 4. Spectra of **1** in the solid state. (a) Excitation spectrum at 77 K for 717 nm emission; (b) emission at 77 K for 445 nm excitation, (c) emission at RT for 445 nm excitation.

We were also interested in the possibility we might detect weak, singlet−triplet low energy absorption bands in the far-red/near-IR spectral region, which might help in the assignment of the emission. However, even at a concentration of 5.7×10^{-3} M in a 10 cm cell we could detect no additional absorption bands from **1** across the wavelength range 700−1000 nm. Any absorption bands in this range, other than the tail of the visible band, must have very low extinction coefficients with ε less than about 1 M^{-1} cm^{-1}.

Excitation and Emission Spectroscopy. Neither compound shows emission in either aerated or nitrogen-purged fluid solution but both show strong emission in the solid state and in organic glasses at 77 K. While the bulk of the emission is in the near-infrared there is enough in the visible, particularly for **1**, for it to be seen as a cherry red glow. Figures 4 and 5 show emission and excitation spectra for solid state samples, while Figure 6 gives these for the compounds dissolved in EDT glass at 77 K. Table 2 collects excitation and emission data. For both compounds emission spectra are broad and asymmetric with the emission maximum of **2** generally shifted about 30 nm to the red compared to that of **1**, consistent with the relative positions of their absorption maxima, and with **1** showing asymmetry with a shoulder to the red of the main band which is at 750 nm while **2** shows a shoulder to the blue of the main band which is at 790 nm. It is interesting to note that in the solid state the emission maximum for **1** at 77 K is shifted about 30 nm

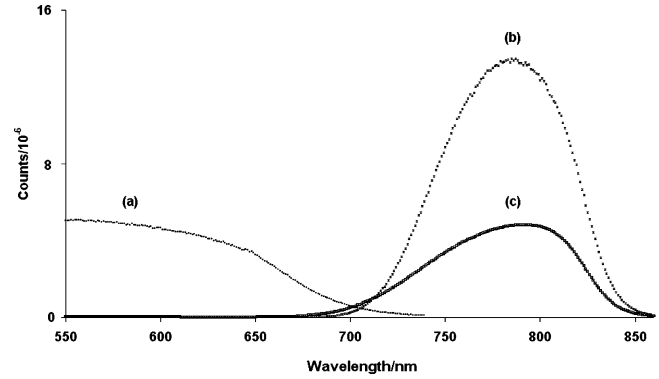

Figure 5. Spectra of **2** in the solid state. (a) Excitation spectrum at 77 K for 785 nm emission; (b) emission at 77 K for 445 nm excitation, (c) emission at RT for 445 nm excitation.

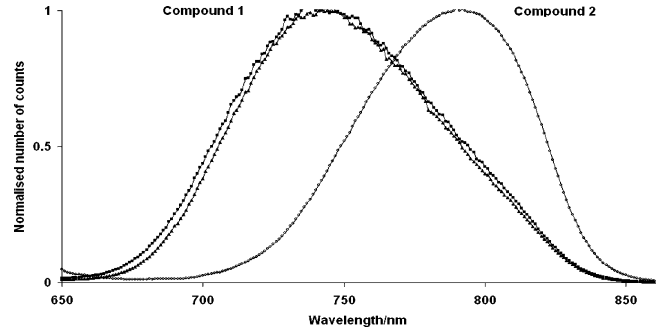

Figure 6. Emission spectra of **1** and **2** in organic glasses at 77 K for 445 nm excitation. **1** in EDT and MCH, **2** in EDT.

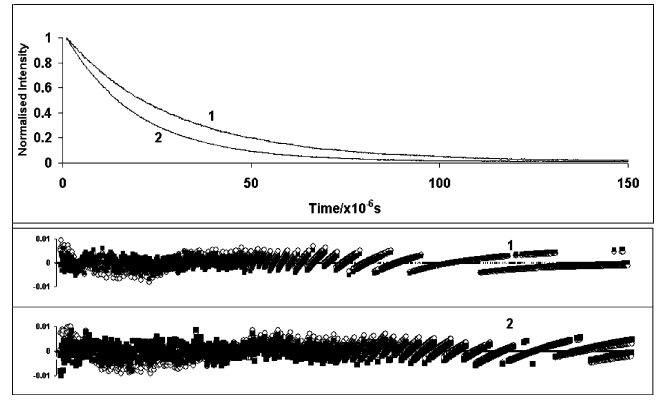

Figure 7. Emission decay curves for **1** and **2** in EDT glass, at 750 and 790 nm, respectively, excitation at 355 nm, with residuals for single exponential (open circles) and double exponential (filled squares) fits. (The aliasing which is apparent in the residuals at long times is a consequence of digitization).

to the red as compared to that at RT, while for **2** the shift is much smaller, about 7 nm, and in the opposite direction. In the solid state at 77 K, excitation spectra show that excitation out to about 650 or 700 nm, for **1** and **2**, respectively, is effective in inducing luminescence. The excitation spectrum of **1** also shows a very weak excitation band at about 620 nm for which a corresponding absorption band has not been detected in solution. As Figure 5 and Table 2 show, excitation spectra in a glass at 77 K are similar in shape to the RT absorption spectra but with excitation maxima shifted about 10 nm compared to RT absorption maxima. Emission spectra are very similar in both MCH glass and the more polar EDT glass, as seen in Figure 6.

Table 2. Lifetime and Quantum Yield Data for **1** and **2** in Various Media[a]

		solid state						organic glass								
			298 K			77 K			EDT			MCH		toluene		
compound	λ_{exc}/nm	λ_{emiss}/nm	τ_0/μs 1st order	τ_0/μs (1+1)[a]	λ_{em}/nm	τ_0/μs 1st order	τ_0/μs (1+1)[a]	λ_{emiss}/nm	τ_0/μs 1st order	τ_0/μs (1+1)[a]	Φ_{emiss}	λ_{emiss}/nm	λ_{emiss}/nm	τ_0/μs 1st order	τ_0/μs (1+1)[a]
1	355	717	1.82 ± 0.12	1.61 (90%) 3.55 (10%)	752	19.1 ± 0.38	19.5 (18%) 15.5 (82%)	742	18.1 ± 0.14	11.5 (27%) 20.1 (83%)	0.12	747	759	18.5 ± 0.11	15.1 (39%) 22.4 (61%)
								789[b]	18.2 ± 0.12	12.1 (29%) 21.2 (81%)					
	532	718	1.84 ± 0.13	1.12 (71%) 3.09 (29%)	752	19.5 ± 0.39	19.7 (20%) 15.6 (80%)	742	18.5 ± 0.18	17.1(87%) 28.1(13%)		747	759	18.3 ± 0.13	16.5 (82%) 28.9 (18%)
								789[b]	18.4 ± 0.14	17.9 (84%) 26.4 (16%)					
2	355	792	6.77 ± 0.25	2.75 (49%) 9.73 (51%)	785	11.6 ± 0.11	8.53 (38%) 13.7 (62%)	790	11.2 ± 0.10	9.11 (76%) 19.3 (24%)	0.13		798	11.6 ± 0.25	8.73 (68%) 18.7 (32%)
								751[b]	11.3 ± 0.13	9.23 (74%) 19.8 (26%)					
	532	792	7.29 ± 0.28	2.72 (47%) 10.2 (53%)	786	11.7 ± 0.12	9.89 (35%) 15.7 (65%)	791 751[b]	11.2 ± 0.10	9.16 (78%) 19.1 (22%)		798		12.1 ± 0.26	8.65 (72%) 18.2 (28%)
									11.3 ± 0.12	9.44 (75%) 19.6 (25%)					

[a] For double exponential, (1+1), curve fits values in brackets are percentage contributions of each decay component. [b] Shoulder to the main peak.

Figure 8. Normalized emission decay curves for **2**. (a) In EDT glass at 77 K: four indistinguishable overlying decay curves, for 750 and 790 nm emission wavelengths each with 532 and 355 nm excitation; (b) in solid state at 77 K: two overlying decay curves, for 532 and 355 nm excitation; and (c,d) solid state at RT: two decay curves, for 532 nm (c) and 355 nm (d) excitation.

Emission quantum yields for solid glasses at 77 K are difficult to determine precisely. We compared emission intensities from **1** and **2** in EDT at 77 K with those from TPP as emission standard in the same EDT solvent at both room temperature and 77 K, using two excitation wavelengths where their room temperature absorption spectra had identical absorbances. This gave emission yields of 0.12 (±0.01) for **1** and 0.13 (±0.01) for **2** in EDT glass at 77 K. We have not attempted to measure solid state quantum yields but note that for both compounds there is a 3−5 fold increase in intensity as the solid is cooled from room temperature to 77 K. Furthermore, based simply on the size of the emission signals obtained, we estimate solid state quantum yields of **1** and **2** at 77 K to be of the same order of magnitude as those obtained in the low temperature glass.

Time Resolved Emission Studies. Table 2 collects kinetic data. For each compound, decay kinetics are the same across the emission band and with either 355 or 532 nm excitation. While for both compounds a double exponential decay is statistically better than a single exponential, the difference between the quality of the two fits for **1** is small, and we prefer this for kinetic analysis for **1**. In the case of **2**, the difference in the quality of the fits is rather more significant, and the fitting parameters obtained by free fitting are generally constant for both excitation wavelengths and emission bands. Figure 7 shows decay curves for **1** and **2** in EDT glass with residuals for single exponential and double exponential fits. Although we have no evidence for more than one chemical species present, there may be a number of local environments or structural conformations in the solid or glass which give a number of lifetimes which together are modeled better by a double exponential than a single exponential decay. For completeness we include fitting parameters for both single and double exponential fits for both compounds in Table 2. For each compound, lifetimes at 77 K are the same whether in the solid state or in the organic glasses, with first order fit lifetimes of $\tau = 18.8$ (±0.7) μs and 11.5 (±0.3) μs for **1** and **2**, respectively (see Figure 8). Combination of these lifetimes with quantum yield

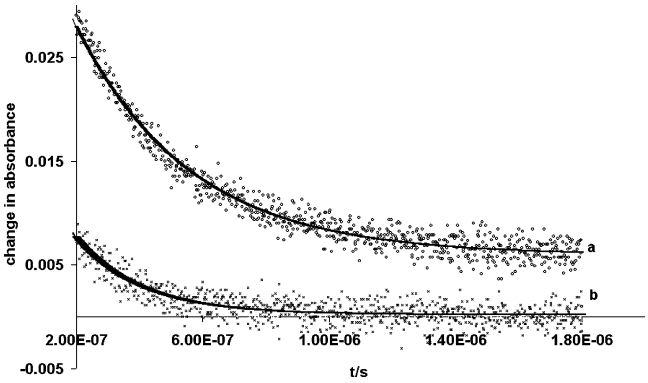

Figure 9. Transient absorbance of **2** in acetonitrile at 420 nm following excitation at 355 nm. (a) Nitrogen purged solution; (b) air-equilibrated solution.

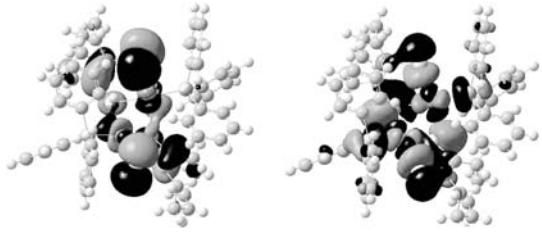

Figure 10. HOMO (left) and LUMO (right) for **2** in the crystal structure geometry. The molecule is aligned so the folded square made from the two Pd atoms and Se3 and Se5 atoms lie in the center of the image (the "Maltese cross" of the top right center Pd orbital is quite distinctive in the LUMO diagram). The triphenyl phosphine groups lie on the diagonal running from bottom left to top right, and the cyclooctene rings are on the diagonal from top left to bottom right. Notable features are as follows. The HOMO diagram shows large orbital lobes on Se4 and Se6 and on the two cyclooctene π orbitals; and there is little involvement of orbitals on the P atoms. The LUMO diagram shows a more diffuse MO with a marked reduction in the orbital lobes on Se4 and Se6, and on C9 and C11 of the -ene carbon atoms; it also shows significant involvement of the P orbitals (the black orbital lobe on the top right P atom in the LUMO is a distinctive feature which can be compared to lack of involvement of the corresponding atom in the HOMO).

data gives radiative lifetimes of 151 ($\pm$13) μs and 86 ($\pm$7) μs for compounds **1** and **2**, respectively, at 77 K in EDT glass. In the solid state at room temperature **1** has a lifetime of 1.83 ($\pm$0.02) μs while for **2** it is 7.0 ($\pm$0.3) μs.

Nanosecond Transient Absorption and Singlet Oxygen Studies. The long emission radiative lifetimes suggest a spin-forbidden transition. Because of this we carried out studies of nanosecond transient absorption in the hope of detecting triplet−triplet absorption. For both compounds no transient absorbances greater than about 0.003 could be detected across the spectral range of 380−620 nm on the nanosecond−microsecond time scale in either fluid EDT or toluene solution, in either the presence or absence of oxygen. However, both compounds do show weak transient absorptions in acetonitrile. For **2** in acetonitrile we detected a very weak transient signal showing a broad absorption across the visible with a maximum at about 420 nm. Both signal size and decay kinetics were oxygen dependent, and Figure 9 shows decay kinetics in the presence and absence of oxygen. In the absence of oxygen the data fit a single exponential decay with rate constant 2.8 ($\pm$0.1) $\times$ 10^6 s^{-1} and significant residual absorption, with relative amplitudes of 86% and 14%. In the presence of oxygen the decay curve fits a single exponential with $k = 4.9$ ($\pm$0.1) $\times$ 10^6 s^{-1} with no significant residual absorption. Compound **1** gives no significant signal in the presence of oxygen, but does give a very broad absorption across the visible with a maximum about 420 nm in nitrogen-purged solution The curve obtained in the absence of oxygen can be fitted to a double exponential with $k_1 =$ 2.0 ($\pm$0.3) $\times$ 10^6 s^{-1}, 64%; and $k_2 = 2.0$ ($\pm$0.2) $\times$ 10^5 s^{-1}, 36%. It is difficult to assign these transients with any certainty, but the signals are not consistent with formation of an oxygen-quenched triplet because the signal amplitudes are oxygen dependent. Perhaps all we can say is that these compounds show some low yield photochemical activity in acetonitrile solution, with either excited state(s) or products which are long enough lived to interact with oxygen. Bearing in mind that these transients are observed in acetonitrile but not in toluene or EDT, it is tempting to suggest they involve charge transfer species. Further evidence for the lack of triplet state formation comes from singlet oxygen studies where we could detect no emission assignable to singlet oxygen across the wavelength range 1200−1350 nm upon 550 nm excitation of either **1** or **2** in air-equilibrated acetonitrile solution. On the basis of previous measurements with the system used, we estimate the quantum yield of singlet oxygen formation, Φ_Δ, to be less than about 5 $\times$ 10^{-4} which we can also take as an upper limit for the quantum yield of any triplet states of significant lifetime.

Table 3. MO Description, Wavelengths, and Oscillator Strengths from DFT Calculations for the Transitions from S_0 to T_1, T_2, S_1 and S_2 for **2** in the Crystal Structure Geometry

transition	contribution	state	wavelength/ nm	oscillator strength
HOMO → LUMO	+0.694	triplet	684	0
(HOMO−1)→ (LUMO+1)	−0.155			
(HOMO−1) → LUMO	+0.632	triplet	629	0
HOMO → (LUMO+1)	−0.308			
HOMO → LUMO	+0.641	singlet	612	0.0156
(HOMO−1)→ (LUMO+1)	−0.213			
(HOMO−1)→ LUMO	+0.624	singlet	586	0.0006
HOMO → (LUMO+1)	−0.274			

Density functional theory (DFT) Calculations. The crystal structure of **2** shows the two planes formed by the ligands coordinated to the two Pd atoms at an angle of about 110° and a relatively short Pd−Pd intramolecular distance (3.08 Å).[25] Results from DFT calculations for the excited states of **2** in this crystal geometry are given in Table 3. The calculations give a pair of reasonably close lying singlet states at 612 and 586 nm, with oscillator strengths of 0.0156 and 0.0006, respectively, and the lowest energy triplet state at 684 nm. Experimentally, the lowest absorption energy level for **2** is at 596 nm with an oscillator strength of 0.019, while the emission maximum is at 785 nm at 77 K (Table 2).

Since the individual atomic orbitals of the Gaussian basis set are not orthogonal the fractional atomic orbital electron character of the molecular orbital (MO) cannot be calculated simply from the square of the atomic orbital coefficient in the molecular orbital.[32] However, a measure of the relative

(32) Clark, T. *A Handbook of Computational Chemistry*; Wiley-Interscience: New York, 1985.

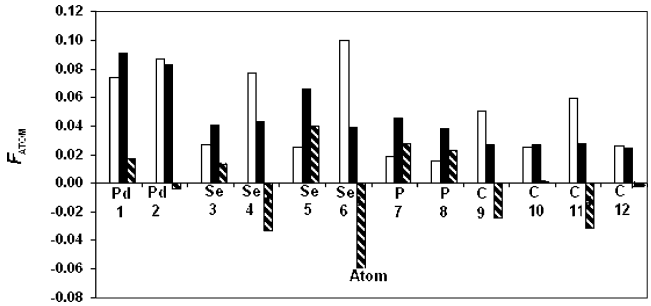

Figure 11. Fractional contribution of the sum of the modulii of the atomic orbital coefficients in the HOMOs (open bars) and LUMOs (filled bars), that is, F_{atom}, for selected atoms. The difference, F_{atom}(LUMO) − F_{atom}(HOMO), is also shown (striped bars) The atomic numbering corresponds to that in Figure 1.

contribution of an atomic orbital is given by the fractional contribution of the modulus of the coefficient in the MO, that is, $F = |c_{(AO)}|/\sum|c_{(AO)}|$,[33] and summation of this term for any atom, F_{atom}, gives some indication of the importance of the atomic orbitals of that atom in the MO. Figure 10 shows the highest occupied molecular orbitals (HOMOs) and the lowest unoccupied molecular orbitals (LUMOs), while Figure 11 gives a histogram of F_{atom} for the Pd, Se, P, and -ene C atoms in both HOMOs and LUMOs together with the difference F_{atom}(LUMO−HOMO). Both MOs are quite diffuse over Pd, Se, and -ene C orbitals but the HOMO has little contribution from P atoms. In the HOMO the main atomic orbital contributions are from Pd, Se (notably Se4 and Se6, see Figure 1 for numbering), and -ene C atoms (notable C9 and C11), with little from P. In contrast, the LUMO has lower involvement of atomic orbitals on Se4 and Se6, and -ene carbons, C9 and C11, but increased contributions from atomic orbitals on P and Se3 and Se5. (The situation for the HOMO−1 to LUMO+1 transition, not shown, is similar). Overall, the DFT calculations suggest a transition involving a shift in orbital character toward increasing P involvement and a reduction in -ene C involvement in the excited state, together with a significant shift in the distribution of involvement from Se4 and Se6 to Se3 and Se5. The increasing involvement of P atomic orbitals in the LUMO (and LUMO+1) orbital is consistent with the observation that the lowest energy absorption maxima of **2** are shifted to higher wavelength compared to those of **1** (Table. 1).

It is interesting to note that optimization of the molecular geometry of the analogous structure where the phosphine phenyl groups are replaced by hydrogens to facilitate calculation[34] gives an essentially planar molecule in which all the Pd, Se, P, and -ene C atoms are essentially co-planar, where the angle between the two Pd ligand planes is about 180°, and where there is no direct Pd−Pd interaction. Excited-state calculations on this structure give transitions of a generally similar nature to those calculated for the crystal structure, but with a pair of close lying singlet−singlet transitions at 877 and 885 nm, and a pair of close lying singlet−triplet transitions at 1134 and 1127 nm. The similarity of absorption and emission behavior in the solid state and frozen solution suggests that, rather than being a consequence of crystal packing, the relatively short Pd−Pd distance and bent Pd ligand planes observed in the crystal structure may be significant structural features which are retained in fluid solution and organic glasses.

Origin of Emission. We assign the emission band to the molecular triplet because of the relatively long lifetime and the significant energy gap between emission and the lowest energy absorption band. The results of the DFT calculations also support this in that the calculations correlate well with the experimental data in terms of lowest singlet energy and transition oscillator strength, and a triplet in the far-red/near-IR. The structure in the emission bands is probably due to emission into two ground-state vibrational levels separated by an energy difference of about 800 cm^{-1} rather than two distinct transitions, because the decay kinetics are the same for both bands.

The failure to detect any triplet−triplet absorption in solution on the nanosecond time scale suggests that either the triplet lifetime is less than about 50 ns in fluid solution, or deactivation of the singlet state goes via a route in which the triplet state is not populated. Furthermore, assuming that any triplet formed can be quenched by oxygen to give singlet oxygen at about the diffusion controlled rate, then the failure to detect singlet oxygen indicates that $\Phi_T \times \tau \leq 50$ ns. Irrespective of whether it is rapid singlet state deactivation without triplet formation or rapid deactivation of the triplet state, the question is what is the nature of this very fast deactivation process; the detection of the triplet in the rigid environment of a glass or crystal suggests it involves molecular torsion.

Conclusions. Compounds **1** and **2** have been shown to give far-red/near-infrared phosphorescence when in the solid state or a rigid organic glass at 77 K. They are, to the best of our knowledge, the first examples of luminescent Pd−Se compounds in the literature. The complexes have radiative lifetimes of 2−7 μs in the solid state at 298 K. At 77 K in the solid state, and in frozen organic glasses, they have observed phosphorescence lifetimes of about 11−20 μs with quantum yields of about 0.12, which gives radiative lifetimes of about 90−160 μs. No emission was detected from either **1** or **2** in fluid solution even when nitrogen-purged; in addition, we could not detect any transient absorption which could be assigned to the triplet state, or any singlet oxygen generation in aerated solution ($\Phi_\Delta \leq 5 \times 10^{-4}$). The fact that this difference in behavior occurs in going from fluid to rigid environments suggests that molecular motion is an effective deactivation route for either the triplet state or its precursor.

DFT calculations give results in general agreement with those experimentally determined in terms of lowest singlet energy and transition oscillator strength, and a triplet state in the far-red/near-IR. The S_0 to S_1 and T_1 transitions show a shift in MO character from one with significant -ene π involvement but very little P involvement in the ground-state to one with less −ene π but greater P involvement in

(33) Foresman, J. B.; Frisch, A. *Exploring Chemistry with Electronic Structure Methods: a Guide to Using Gaussian*; Gaussian Inc.: Pittsburgh, 1993.
(34) Basque, R.; Maseras, F. *J. Comput. Chem.* **2002**, *21*, 562–571.

the excited states; there is also a significant shift in the distribution of involvement of atomic orbitals on the four Se atoms.

Acknowledgment. We would like to thank the EPSRC National Mass Spectrometry Service Centre, Swansea University; the staff of the Departmento de Quimica, Universidade de Coimbra, Portugal (particularly C. Serpa, J. Pina, and H. D. Burrows), for use of, and help with, their ns flash photolysis, SPEX spectrometer, and singlet oxygen detection systems; Swansea University (KR, JGP, CAW), EPSRC (KR) and Kodak European Research (JGP) for financial support; and Johnson Matthey plc for the loan of Pd salts under their University Loan Scheme.

IC801694R